

Bright Flares in Supergiant Fast X-ray Transients

N. Shakura¹ \star , K. Postnov¹, L. Sidoli², A. Paizis²

¹ Sternberg Astronomical Institute, Moscow M.V. Lomonosov State University, Universitetskij pr., 13, 119992, Moscow, Russia

² INAF, Istituto di Astrofisica Spaziale e Fisica Cosmica, Via E. Bassini 15, I-20133 Milano, Italy

Received ... Accepted ...

ABSTRACT

At steady low-luminosity states, Supergiant Fast X-ray Transients (SFXTs) can be at the stage of quasi-spherical settling accretion onto slowly rotating magnetized neutron stars from the OB-companion winds. At this stage, a hot quasi-static shell is formed above the magnetosphere, the plasma entry rate into magnetosphere is controlled by (inefficient) radiative plasma cooling, and the accretion rate onto the neutron star is suppressed by a factor of ~ 30 relative to the Bondi-Hoyle-Littleton value. Changes in the local wind velocity and density due to, e.g., clumps, can only slightly increase the mass accretion rate (a factor of ~ 10) bringing the system into the Compton cooling dominated regime and led to the production of moderately bright flares ($L_x \lesssim 10^{36}$ erg/s). To interpret the brightest flares ($L_x > 10^{36}$ erg/s) displayed by the SFXTs within the quasi-spherical settling accretion regimes, we propose that a larger increase in the mass accretion rate can be produced by sporadic capture of magnetized stellar wind plasma. At sufficiently low accretion rates, magnetic reconnection can enhance the magnetospheric plasma entry rate, resulting in copious production of X-ray photons, strong Compton cooling and ultimately in unstable accretion of the entire shell. A bright flare develops on the free-fall time scale in the shell, and the typical energy released in an SFXT bright flare corresponds to the mass of the shell. This view is consistent with the energy released in SFXT bright flares ($\sim 10^{38} - 10^{40}$ ergs), their typical dynamic range (~ 100), and with the observed dependence of these characteristics on the average unflaring X-ray luminosity of SFXTs. Thus the flaring behaviour of SFXTs, as opposed to steady HMXBs, may be primarily related to their low X-ray luminosity allowing sporadic magnetic reconnection to occur during magnetized plasma entry into the magnetosphere.

Key words: accretion - pulsars:general - X-rays:binaries

1 INTRODUCTION

Supergiant Fast X-ray Transients (SFXTs) are a subclass of High-Mass X-ray Binaries (HMXBs) associated with early-type supergiant companions (Pellizza, Chaty & Negueruela 2006, Chaty et al. 2008, Rahoui et al. 2008), and characterized by sporadic, short and bright X-ray flares reaching peak luminosities of 10^{36} – 10^{37} erg s⁻¹. Most of them were discovered by INTEGRAL (Molkov et al. 2003; Sunyaev et al. 2003; Grebenev, Lutovinov & Sunyaev 2003, Sguera et al. 2005, Negueruela et al. 2006). They show high dynamic ranges (between 100 and 10,000, depending on the specific source; e.g. Romano et al. 2011, 2014) and their X-ray spectra in outburst are very similar to accreting pulsars in HMXBs. In fact, a half of them have measured neutron star (NS) spin periods similar to those observed from persistent HMXBs (see Sidoli 2012 for a recent review).

The physical mechanism driving their transient behavior, related with the accretion by the compact object of matter from the

supergiant wind, has been discussed by several authors and it is still a matter of debate, as some of them require particular properties of the compact objects hosted in these systems (Grebenev & Sunyaev 2007, Bozzo, Falanga & Stella 2008), and others assume peculiar clumpy properties of the supergiant winds and/or orbital characteristics (in't Zand 2005; Walter & Zurita Heras 2007; Sidoli et al. 2007; Negueruela et al. 2008; Ducci et al. 2009; Oskinova, Feldmeier & Kretschmar 2012).

Recently, a new approach has been proposed from the observational point of view: cumulative luminosity distributions of SFXTs emission have been built for the first time in hard X-rays using the long based *INTEGRAL* public archive (~ 9 years of IBIS data, Paizis & Sidoli 2014). This work enables a self consistent overview of all currently known SFXTs, with quantitative information on source duty cycles, range of variability and shape of the hard X-ray luminosity distributions, especially compared to persistent systems.

In this paper we propose an alternative mechanism for bright flares in SFXTs, which is based on an instability of the quasi-spherical shell around the magnetosphere of a slowly rotating NS. Such shell must be formed at low mass accretion rates \lesssim

\star E-mail: nikolai.shakura@gmail.com, kpostnov@gmail.com

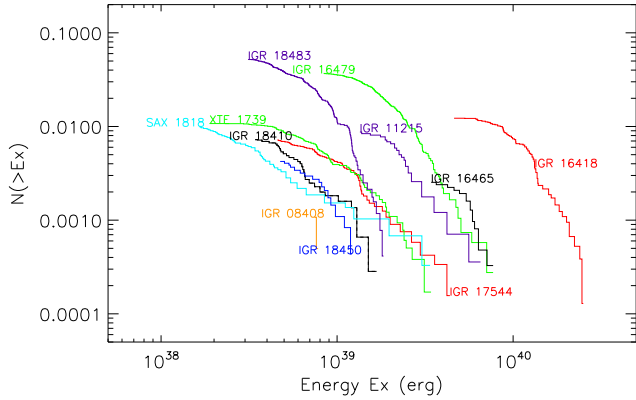


Figure 1. Cumulative distribution of the total energy released in SFXT flares (*INTEGRAL*/*IBIS* data, 17–50 keV). The fraction of time (*y*-axis) spent by SFXTs above a certain energy value (*x*-axis) is given.

$4 \times 10^{16} \text{ g s}^{-1}$ (low accretion X-ray luminosities $\lesssim 4 \times 10^{36} \text{ erg s}^{-1}$) in quasi-spherical accretion from stellar wind of the optical companion (Shakura et al. 2012). In this model, the actual accretion rate through the magnetosphere is controlled by the plasma cooling. (Compton at higher luminosities or radiative at lower ones). The switch from Compton to inefficient radiation cooling is expected to occur at luminosities $\lesssim 10^{35} \text{ erg s}^{-1}$ (Shakura, Postnov & Hjalmarsdotter 2013), resulting in actual accretion rates typically a factor of ~ 30 smaller than the maximum possible Bondi-Hoyle-Littleton rate determined by the stellar wind properties and NS orbital velocity. Variations in the stellar wind velocity and density are translated into plasma density changes near the magnetosphere and hence, via cooling, into the X-ray luminosity variations. Above some accretion rate, the restructure of X-ray beam pattern from NS can bring the source into more effective Compton cooling regime, resulting in a moderate flare with $L_x \lesssim 10^{36} \text{ erg s}^{-1}$. To explain the bright SFXT flares, however, a much more efficient plasma entry rate is required, signaling an instability in the shell. We suggest that the instability can be triggered by the sudden increase in the mass accretion rate through the magnetosphere due to reconnection of the large-scale magnetic field sporadically carried by the stellar wind of the optical OB companion. We show that this instability can reproduce the observed energy released in bright flares of SFXTs, as well as the dynamic range of the flares and their dependence on the mean unflaring X-ray luminosity in different sources. The bright flares due to the proposed mechanism can occur on top of smooth variation of mass accretion rate due to, for example, orbital motion of the neutron star in a binary system.

2 ENERGY RELEASED IN SFXT FLARES

Given the rare, sporadic and intermittent character of the bright flares in SFXTs (usually, single outbursts are separated by several months of either much fainter X-ray emission or quiescence), the exploitation of very long based archival data is the best strategy to obtain reliable quantitative information about the source duty cycles, X-ray range of variability, shape of the luminosity distributions.

The temporal profiles of SFXT flares are usually very complex

and it is not straightforward to define or disentangle an X-ray flare. However, since time scales of flare durations are roughly consistent with *INTEGRAL* pointing durations (order of ks), we consider the single pointing detections as a good representation of SFXT flares.

The energy released during SFXT flares, as observed by *INTEGRAL*, is shown in Figure 1. The plot is an overview of all known SFXTs¹. The data selection and analysis is discussed in detail in Paizis & Sidoli (2014), together with the assumed distances and relevant references, so we refer the reader to that paper for the technical details. In Figure 1, for each source we built the complementary cumulative distribution function of the obtained X-ray flare energies. In each point of these functions, at a given energy E_x (erg), the sum of all events (detections) with an energy larger than E_x are plotted. The energy released in each flare is obtained by multiplying the flare luminosities as obtained in Paizis & Sidoli (2014), Figure 3, by the duration of the pointings.

Each curve has been normalised to the total exposure of the source fields observed by *IBIS*, hence they can be directly compared: the energy released during flares by SAX J1818.6–1703 is $> 1.7 \times 10^{38} \text{ ergs}$ for about 1% of the total observing time (7.3 Ms), whereas the energy released in IGR J18483–0311 flares is higher than $3.1 \times 10^{38} \text{ ergs}$ for 5% of the total observing time (6.0 Ms). The lower end of the curves (i.e. towards dimmer flares) is limited by the *IBIS*/*ISGRI* sensitivity in a single pointing.

3 MODEL OF SFXT BRIGHT FLARES

3.1 Settling subsonic accretion onto slowly rotating NS

There can be two distinct cases of quasi-spherical accretion onto slowly rotating magnetized NS. The classical Bondi-Hoyle-Littleton accretion takes place when the shocked matter rapidly cools down (via Compton cooling), and the matter freely falls toward the NS magnetosphere. A shock in the accreting plasma is formed at some distance above the magnetosphere. Close to the magnetopause, the shocked matter rapidly cools down and enters the magnetosphere via Rayleigh-Taylor instability Arons & Lea (1976). The magnetospheric boundary is characterized by the Alfvén radius R_A , which can be calculated from the balance of the ram pressure of the infalling matter and the magnetic field pressure at the boundary. This regime of quasi-spherical accretion is realized in bright X-ray pulsars with $L_x > 4 \times 10^{36} \text{ erg s}^{-1}$ (Shakura et al. 2012).

If the shocked matter remains hot (when plasma cooling time is much longer than the free-fall time, $t_{cool} \gg t_{ff}$), a hot quasi-static shell with almost iso-angular momentum distribution forms above the magnetosphere. The subsonic (settling) accretion sets in. The shell mediates the angular momentum transfer from/to the NS magnetosphere via viscous stresses due to convection. In this regime, the mean radial velocity of matter in the shell u_r is smaller than the free-fall velocity u_{ff} : $u_r = f(u)u_{ff}$, $f(u) < 1$, and is determined by the plasma cooling rate near the magnetosphere: $f(u) \sim [t_{ff}(R_A)/t_{cool}(R_A)]^{1/3}$. Here the actual mass accretion rate onto NS can be significantly smaller than the Bondi mass accretion rate, $\dot{M}_a = f(u)\dot{M}_B$. The settling accretion is expected to occur at

¹ IGR J17544–2619, IGR J16418–4532, IGR J16479–4514, IGR J16465–4507, SAX J1818.6–1703, IGR J18483–0311, XTE J1739–302, IGR J08408–4503, IGR J18450–0435, IGR J18410–0535, IGR J11215–5952

$L_x < 4 \times 10^{36}$ erg s⁻¹ (see Shakura et al. 2012, 2013, 2014 for the detailed derivation, discussion and applications to spin-up/spin-down of slowly rotating low-luminosity X-ray pulsars).

Different regimes of plasma cooling near the magnetosphere (radiative or Compton) can take place. The switch-off of the Compton cooling is expected with decreasing X-ray luminosity, which can be related to X-ray beam generated near the NS surface switching from fan-like to pencil-like form, as discussed in Shakura, Postnov & Hjalmarsdotter (2013) with regard to temporal appearance of low-luminosity 'off' states in Vela X-1. The pulse profile phase change associated with X-ray beam switching below some critical luminosity, as observed in Vela X-1, seems to be suggested by an *XMM-Newton* observation of the SFXT IGR J11215–5952 (see Fig. 3 in Sidoli et al. (2007)), corroborating the subsonic accretion regime with radiative plasma cooling at low X-ray luminosities in SFXTs as well.

3.2 Energy released in bright flares

Fig. 1 suggests that the typical energy released in a SFXT bright flare is about $10^{38} - 10^{40}$ ergs, varying by one order of magnitude for different sources. That is, the mass fallen onto the NS in the typical bright flare varies from 10^{18} g to around 10^{20} g. (assuming an X-ray emission efficiency of about 0.1).

The typical X-ray luminosity outside outbursts in SFXTs is about $L_{x,low} \approx 10^{34}$ erg s⁻¹ (Sidoli et al. 2008), and below we shall normalise the luminosity to this value, L_{34} . At these small X-ray luminosities, plasma entry rate into magnetosphere is controlled by radiative plasma cooling. Next, it is convenient to normalise the typical stellar wind velocity from hot OB-supergiants v_w to 1000 km s⁻¹ (for orbital periods about few days and larger the NS orbital velocities can be neglected compared to the stellar wind velocity from the OB-star), so that the Bondi gravitational capture radius is $R_B = 2GM/v_w^2 = 4 \times 10^{10} v_8^{-2}$ cm for a fiducial NS mass of $M_x = 1.5M_\odot$.

Consider a quasi-static shell hanging over the magnetosphere around the NS, with the magnetospheric accretion rate being controlled by the radiative plasma cooling. We denote the actual steady-state accretion rate as \dot{M}_a so that the observed X-ray steady-state luminosity is $L_x = 0.1\dot{M}_a c^2$. Then from the theory of subsonic quasi-spherical accretion (Shakura et al. 2012) we know that the factor $f(u)$ (the ratio of the actual velocity of plasma entering the magnetosphere due to the Rayleigh-Taylor instability to the free-fall velocity at the magnetosphere, $u_{ff}(R_A) = \sqrt{2GM/R_A}$) reads (Shakura, Postnov & Hjalmarsdotter 2013; Shakura et al. 2014)

$$f(u)_{rad} \approx 0.036 L_{34}^{2/9} \mu_{30}^{2/27}. \quad (1)$$

Here $\mu_{30} = \mu/10^{30}$ G cm³ is the NS dipole magnetic moment; note a very weak dependence on the NS magnetic field.

The shell is quasi-static (likely convective), unless something triggers much faster matter fall through the magnetosphere (see below the possible reason). It is straightforward to calculate the mass of the shell using the density distribution $\rho(R) \propto R^{-3/2}$ (Shakura et al. 2012). Using the mass continuity equation to eliminate the density above the magnetosphere, we readily find

$$\Delta M \approx \frac{2}{3} \frac{\dot{M}_a}{f(u)} t_{ff}(R_B). \quad (2)$$

Note that this mass can be expressed through measurable values $L_{x,low}$, μ_{30} and the (directly unobserved) stellar wind velocity at the Bondi radius $v_w(R_B)$. Using Eq. (1) for radiative plasma cooling, we obtain

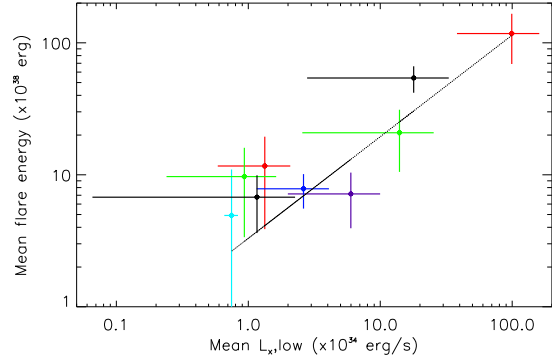


Figure 2. The mean energy released in bright flares (17 – 50 keV, data from Paizis & Sidoli (2014)) versus average *INTEGRAL/IBIS* source luminosity. The average luminosities have been obtained by the source fluxes measured in time-averaged maps Krivonos et al. (2012) (17–60 keV, IBIS survey over 9 years, nine SFXTs). The same distances used to derive our flare energies have been considered for the estimates of the average luminosities. Sources are colored as in Fig. 1. Errors shown are explained in text. The *x-axis* is in units of 10^{34} erg s⁻¹, the *y-axis* is in units of 10^{38} ergs. The straight line gives the formal rms linear fit with the slope 0.77 ± 0.13 .

$$\Delta M_{rad} \approx 8 \times 10^{17} [g] L_{34}^{7/9} v_8^{-3} \mu_{30}^{-2/27}. \quad (3)$$

The simple estimate (3) shows that for the likely wind velocity near the NS about 500 km s⁻¹ the *typical* mass of the hot magnetospheric shell is around 10^{19} g, corresponding to 10^{39} ergs released in a flare in which all the matter from the shell is accreted onto the NS, as observed (see Fig. 1). Clearly, the wind velocity variations in different sources by factor ~ 2 would produce a one-order-of-magnitude spread in ΔM observed in bright SFXT flares.

In Fig. 2 we show the mean energy of SFXT bright flares $\Delta E = 0.1\Delta M c^2$ as a function of low (unflaring) X-ray luminosity for sources from Fig. 1. The low (unflaring) X-ray luminosity (*x-axis*) has been taken from Krivonos et al. (2012), where a nine year time-averaged source flux in the 17–60 keV band is given for each source (with the exception of two, IGR J11215–5952 and IGR J08408–4503)². The uncertainties on the low luminosities include both the statistical errors on source fluxes, as reported in Krivonos et al. (2012), and the known SFXTs distances and their uncertainties as reported by Paizis & Sidoli (2014). For clarity, we assumed an uncertainty of 1 kpc for all SFXTs except for SAX J1818.6–1703 (for which we used 0.1 kpc), IGR J16465–4507 and IGR J16418–4532 (4 kpc), IGR J16479–4514 (2 kpc) and IGR J18410–0535 (1.5 kpc). The errors on the *y-axis* in Fig. 2 are based on the standard deviation of the bright flare energies, giving a conservative idea of the range of variability of bright flare energy as observed by *INTEGRAL*. The formal rms fit to these points gives the dependence of $\Delta E_{38} = (3.3 \pm 1.0) L_{34}^{0.77 \pm 0.13}$. This exactly corresponds to radiative cooling regime (see Eq. (3)), as expected. Comparison with coefficient in formula (3) suggests $v_8 \sim 0.62$, the typical wind velocities observed in HMXBs.

What can trigger the SFXT flaring activity? As noted in Shakura, Postnov & Hjalmarsdotter (2013), if there is an instability

² We chose these data as a representation of the non-flaring activity to be compared to our flare detections (Figure 1) because our energy range (17–50 keV) and data sample (~ 9 years) basically overlap (most of the emission from SFXTs is below 50 keV), while Bird et al. (2010) adopt a slightly different energy range (20–40 keV band) and include less data

leading to rapid matter fall through the magnetosphere, a lot of X-ray photons produced near the NS surface should rapidly cool down the plasma, further increasing the plasma fall velocity through magnetosphere and the ensuing accretion NS luminosity. Therefore, in a bright flare the entire shell can fall onto the NS on the free-fall time scale from the outer radius of the shell $t_{ff}(R_B) \sim 1000$ s. Clearly, the shell will be replenished by new wind capture, so the flares will repeat as long as the rapid mass entry rate into the magnetosphere is sustained.

3.3 Magnetized stellar wind as the flare trigger

Observations suggest that about $\sim 10\%$ of hot OB-stars have magnetic fields up to a few kG (see Donati & Landstreet (2009); Braithwaite (2013) for a review and discussions). The fields of massive stars affect their winds rather than their near-surface distribution of chemical elements and are capable of reshaping the wind by forcing the escaping plasma to follow the field lines. This results in a complex variable wind structure around a rotating magnetized star (see, for example, the analysis of X-ray observations and MHD-simulations of the wind around young magnetic O-star θ^1 Orionis C in Gagné et al. (2005)). According to such calculations, within the Alfvén radius of the star, where the wind flow is dominated by the large-scale magnetic field of the star, the wind tends to flow into star’s magnetic equatorial plane, producing shocks and prominence-like structures; farther away the flow can carry close loops of magnetic fields, much like in the Solar wind. Magnetic spots on the surface of hot stars might also be responsible for variable magnetic stellar wind activity and clumping (Cantiello & Braithwaite 2011). In a detached binary system, the wind structure can be even more complicated, as the OB-companion is likely to be non corotating with the orbital period and may have the spin axis inclined to the orbital plane (due to, e.g., the natal kick acquired by the NS during the formation in supernova explosion). Therefore, it is possible that the wind material lost by the supergiant companions of SFXTs is non-magnetized for most of the time, and only sporadically it transports with it part of the star magnetic field. The shell instability described above can be triggered by large-scale magnetic field sporadically carried by the stellar wind of the optical OB companion.

It is also well known from Solar wind studies (see e.g. reviews Zelenyi & Milovanov (2004); Bruno & Carbone (2013) and references therein) that the Solar wind patches carrying tangent magnetic fields has a lower velocity (about 350 km s^{-1}) than the wind with radial magnetic fields (up to $\sim 700 \text{ km s}^{-1}$). Fluctuations of the stellar wind density and velocity from massive stars are also known from spectroscopic observations (Puls, Vink & Najarro 2008), with the typical velocity fluctuations up to $0.1 v_\infty \sim 200 - 300 \text{ km s}^{-1}$.

The effect of the magnetic field carried by the stellar wind is twofold: first, it can trigger rapid mass entry rate to the magnetosphere via magnetic reconnection in the magnetopause (the phenomenon well known in the dayside Earth magnetosphere, Dungey (1961)), and second, the magnetized clumps with tangent magnetic field have smaller velocity than unmagnetized ones (or carrying the radial field). The first factor, under certain conditions discussed below, can increase the plasma fall velocity in the shell from inefficient, radiative-cooling controlled settling accretion with $f(u)_{rad} \sim 0.03 - 0.1$, up to the maximum possible free-fall velocity with $f(u) = 1$. In other words, during the bright flare the subsonic settling accretion transforms into the supersonic Bondi accretion. The second factor (slower wind velocity in magnetized clumps with tangent magnetic field) strongly increases the Bondi

radius $R_B \propto v_w^{-2}$ and the corresponding Bondi mass accretion rate $\dot{M}_B \propto v_w^{-3}$. Thus, we suggest that should a magnetized density clump be captured, the magnetic reconnection can trigger the shell instability around the NS magnetosphere.

To substantiate these factors, let us write down the mass accretion rate onto the NS in the unflaring (low-luminosity) state as $\dot{M}_{a,low} = f(u)\dot{M}_B$ with $f(u)$ given by formula (1) and $\dot{M}_B \approx \pi R_B^2 \rho_w v_w$. Eliminating the wind density ρ_w using the mass continuity equation written for the spherically symmetric stellar wind from the optical star with power \dot{M}_o and by assuming circular binary orbit, we arrive at $\dot{M}_B \approx \frac{1}{4} \dot{M}_o \left(\frac{R_B}{a}\right)^2$. Next, let us exploit the well-known relation for the radiative wind mass-loss rate from massive hot stars $\dot{M}_o \approx \epsilon \frac{L}{c v_\infty}$ where L is the optical star luminosity, v_∞ is the stellar wind velocity at infinity, typically $2000 - 3000 \text{ km s}^{-1}$ for OB stars, $\epsilon \approx 0.4 - 1$ is the efficiency factor (Lamers, van den Heuvel & Petterson 1976) (in the numerical estimates below we shall assume $\epsilon = 0.5$). It is also possible to reduce the luminosity L of a massive star to its mass M using the phenomenological relation $(L/L_\odot) \approx 19(M/M_\odot)^{2.76}$ (see e.g. Vitrichenko, Nadyozhin & Razinkova (2007)). Combining above equations and using third Kepler’s law to express the orbital separation a through the binary period P_b , we find for the X-ray luminosity of SFXT in the non-flaring state

$$L_{x,low} \approx 5 \times 10^{35} [\text{erg s}^{-1}] f(u) \left(\frac{M}{10 M_\odot}\right)^{2.76-2/3} \left(\frac{v_\infty}{1000 \text{ km s}^{-1}}\right)^{-1} \left(\frac{v_w}{500 \text{ km s}^{-1}}\right)^{-4} \left(\frac{P_b}{10 \text{ d}}\right)^{-4/3}, \quad (4)$$

which for $f(u) \sim 0.03 - 0.1$ corresponds to the typical low-state luminosities of SFXTs $\sim 10^{34} \text{ erg s}^{-1}$.

It is straightforward to see that the transition from the low state (subsonic accretion with slow magnetospheric entry rate $f(u) \sim 0.03 - 0.1$) to the supersonic free-fall Bondi accretion with $f(u) = 1$ due to the magnetized stellar wind with the velocity decreased by factor two, for example, would lead to a flare luminosity of $L_{x,flare} \sim (10 \div 30) \times 2^5 L_{x,low}$. This shows that the dynamical range of SFXT bright flares ($\sim 300 - 1000$) can be naturally reproduced by the proposed mechanism.

For magnetic field reconnection to occur, the time the magnetized plasma spends near the magnetopause should be at least comparable to the reconnection time, $t_r \sim R_A/v_r$, where v_r is the magnetic reconnection rate, which is difficult to assess from the first principles (Zweibel & Yamada 2009). For example, in the Petschek fast reconnection model $v_r = v_A(\pi/8 \ln S)$, where v_A is the Alfvén speed and S is the Lundquist number (the ratio of the Ohmic diffusion time to the Alfvén time); for typical conditions near NS magnetospheres we find $S \sim 10^{28}$ and $v_r \sim 0.006 v_A$. In real astrophysical plasmas the large-scale magnetic reconnection rate can be a few times as high, $v_r \sim 0.03 - 0.07 v_A$ (Zweibel & Yamada 2009), and, guided by phenomenology, we can parametrize it as $v_r = \epsilon_r v_A$ with $\epsilon_r \sim 0.01 - 0.1$. The longest time-scale the plasma penetrating into the magnetosphere spends near the magnetopause is the instability time, $t_{inst} \sim t_{ff}(R_A) f(u)_{rad}$ (Shakura et al. 2012), so the reconnection can occur if $t_r/t_{inst} \sim (u_{ff}/v_A)(f(u)_{rad}/\epsilon_r) \lesssim 1$. As near R_A (from its definition) $v_A \sim u_{ff}$, we arrive at $f(u)_{rad} \lesssim \epsilon_r$ as the necessary reconnection condition. By Eq. (1), it is satisfied only at sufficiently low X-ray luminosities, pertinent to ‘quiet’ SFXT states. *This explains why in HMXBs with convective shells and higher luminosity (but still smaller than $4 \times 10^{36} \text{ erg s}^{-1}$, where the settling accretion is possible), the reconnection from magnetized plasma accretion will not lead to the shell instability, but only to temporal establishing of the ‘strong coupling regime’ of angular momentum transfer through the shell, as discussed in Shakura et al.*

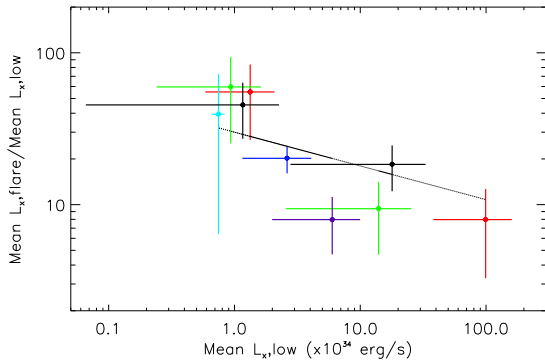


Figure 3. The mean dynamic range of SFXT bright flares $L_{x,flare}/L_{x,low}$ as a function of low (unflaring) X-ray luminosity for sources from Fig. 1 with errors shown as explained in text. Sources are colored as in Fig. 1. The x -axis is in units of 10^{34} erg s^{-1} . The straight line shows the expected dependence (5).

(2012). Episodic strong spin-ups, not associated with strong X-ray flux variations, as observed in GX 301-2, can be manifestations of such ‘failed’ reconnection-induced shell instability³.

Therefore, it seems likely that the key (distinctive) difference between steady HMXBs like Vela X-1, GX 301-2 (showing only moderate flaring activity) and SFXTs is that in the first case the effects of possible magnetized stellar winds from optical OB-companions are insignificant (basically due to rather high accretion rate), while in SFXTs with lower ‘steady’ X-ray luminosity, large-scale magnetic field, sporadically carried by the wind clumps, can trigger SFXT flaring activity via magnetic reconnection near the magnetospheric boundary. The observed power-law SFXT flare distributions, discussed in Paizis & Sidoli (2014), with respect to the log-normal distributions for classical HMXBs (Fürst et al. 2010), may be related to the properties of magnetized stellar wind and physics of its interaction with the NS magnetosphere.

4 DISCUSSION AND CONCLUSIONS

The actually observed dynamic range of bright flares in SFXTs may be higher than 1000. The ratio between L_x at the peak of some bright flares, which can be as high as a few $\times 10^{36}$ erg s^{-1} , sometimes up to 10^{37} erg s^{-1} , and the L_x in the non-flaring state (the weakest L_x ever measured in a couple of SFXTs is $L_{x,low} = 10^{32}$ erg s^{-1}), can reach 10^5 . This very high dynamic range is observed, for example, in IGR 17544-2619 (in’t Zand 2005, Rampy, Smith & Negueruela 2009).

Flares in SFXTs exhibit a rich phenomenology, including single outbursts (like in IGR J18410-0535) or several successive flares on top of a varying base flux (like in IGR J11215–5952, Romano et al. (2009)). In the quasi-spherical accretion model discussed above, the dependence of the quiescent luminosity on the wind velocity is very high, $L_{x,low} \sim v_w^{-5}$ (see Eq. (4) above). This means that in a steady state smooth velocity variations by a factor of two (for example, due to high orbital eccentricity) could change the

X-ray luminosity between the flares by a factor of 30. If the magnetized clumps are sporadically appear in the stellar wind, flares on top of smoothly varying $L_{x,low}$ are expected to occur with the amplitude

$$L_{x,flare}/L_{x,low} \sim f(u)_{rad}^{-1} \sim 30L_{34}^{-2/9} \quad (5)$$

This may be the case of IGR J11215–5952 (Romano et al. 2009). Thus, the stronger wind velocity variations in low-luminosity sources could produce higher dynamic range of flares.

In Fig. 3 we plot the mean dynamic range of bright SFXT flares $L_{x,flare}/L_{x,low}$ as a function of $L_{x,low}$ for sources from Fig. 1. The errors on the x -axis (mean $L_{x,low}$) are calculated as in Fig. 2, while the uncertainties on y -axis, the ratio of the luminosities, are obtained considering the standard deviation from the mean flare luminosity (for $L_{x,flare}$) and the statistical errors for $L_{x,low}$. The solid line shows the expected model dependence according to Eq. (5).

The proposed mechanism of SFXT bright flares is of course highly simplified. For example, the binary orbit can be eccentric, the properties of magnetized winds from OB-supergiants can be anisotropic (see, e.g., model calculations in ud-Doula & Owocki (2002) and other works of those authors), the shells can be not spherically symmetric, the photon field is definitely not spherically symmetric, etc. Nevertheless, the naturalness of the energy and time scales of bright flares, their dynamic range and the dependence of these properties on the unflaring X-ray luminosity seem to be highly suggestive. The observed spread in SFXT flare luminosity and energy distribution (Paizis & Sidoli (2014) and Fig. 1 in the present paper) can be due to the complexity and diversity of the magnetic field reconnection near the magnetopause and variations of the stellar wind properties.

We conclude that the SFXT bright flares can be caused by sporadic transitions between different regimes of accretion in a quasi-spherical shell around a slowly rotating magnetized neutron star. The non-flaring steady states of SFXTs with low X-ray luminosity $L_{x,low} \sim 10^{32} - 10^{34}$ erg s^{-1} may be associated with settling subsonic accretion mediated by ineffective radiative plasma cooling near the magnetospheric boundary. This regime is supported by observations of the X-ray pulse profile phase shift below some X-ray luminosity in XMM-Newton observations of the SFXT IGR J11215–5952 (Sidoli et al. 2007). At this stage, the accretion rate onto the neutron star is suppressed by a factor of ~ 30 relative to the Bondi-Hoyle-Littleton value. Changes in the local wind velocity and density due to, e.g., clumps, can only slightly increase the mass accretion rate (a factor of ~ 10) bringing the system into the Compton cooling dominated regime and led to the production of moderately bright flares ($L_x \lesssim 10^{36}$ erg/s). To interpret the brightest flares ($L_x > 10^{36}$ erg/s) displayed by the SFXTs within the quasi-spherical settling accretion regimes, we propose that a larger increase in the mass accretion rate can be produced by sporadic capture of magnetized stellar wind plasma. Such episodes should not be associated with specific binary orbital phases, as observed in e.g. IGR J17544-2619 (Drave et al. 2014). At sufficiently low accretion rates, magnetic reconnection can enhance the magnetospheric plasma entry rate, resulting in copious production of X-ray photons, strong Compton cooling and ultimately in unstable accretion of the entire shell. A bright flare develops on the free-fall time scale in the shell, and the typical energy released in an SFXT bright flare corresponds to the entire mass of the shell. This view is consistent with the energy released in SFXT bright flares ($\sim 10^{38} - 10^{40}$ ergs), their typical dynamic range (~ 100), and with the observed dependence of these characteristics on the average unflaring X-ray luminosity of SFXTs. Thus the flaring behaviour of

³ See Ikhsanov & Finger (2012) for an alternative explanation of strong spin-ups in GX 301-2 in the frame of another theory of magnetic accretion.

SFXTs, as opposed to steady HMXBs, may be primarily related to their low X-ray luminosity in the settling accretion regime, allowing sporadic magnetic reconnection to occur during magnetized plasma entry the NS magnetosphere.

5 ACKNOWLEDGEMENTS

The authors thank the anonymous referee for notes and A. Lutovinov and B.V. Somov for discussions. NSh acknowledges the Russian Science Foundation grant 14-02-00146. KP was supported by the RFBR grant 14-02-00657a. AP and LS acknowledge the Italian Space Agency financial support *INTEGRAL* ASI/INAF agreement n. 2013-025.R.0.

REFERENCES

- Arons J., Lea S. M., 1976, *ApJ*, 207, 914
 Bird A. J. et al., 2010, *ApJ Suppl.*, 186, 1
 Bozzo E., Falanga M., Stella L., 2008, *ApJ*, 683, 1031
 Braithwaite J., 2013, *ArXiv e-prints*
 Bruno R., Carbone V., 2013, *Living Reviews in Solar Physics*, 10
 Cantiello M., Braithwaite J., 2011, *A&A*, 534, A140
 Chaty S., Rahoui F., Foellmi C., Tomsick J. A., Rodriguez J., Walter R., 2008, *A&A*, 484, 783
 Donati J.-F., Landstreet J. D., 2009, *ARAA*, 47, 333
 Drave S. P., Bird A. J., Sidoli L., Sguera V., Bazzano A., Hill A. B., Goossens M. E., 2014, *MNRAS*, 439, 2175
 Ducci L., Sidoli L., Mereghetti S., Paizis A., Romano P., 2009, *MNRAS*, 398, 2152
 Dungey J. W., 1961, *Physical Review Letters*, 6, 47
 Fürst F. et al., 2010, *A&A*, 519, A37
 Gagné M., Oksala M. E., Cohen D. H., Tonnesen S. K., ud-Doula A., Owocki S. P., Townsend R. H. D., MacFarlane J. J., 2005, *ApJ*, 628, 986
 Grebenev S. A., Lutovinov A. A., Sunyaev R. A., 2003, *The Astronomer's Telegram*, 192, 1
 Grebenev S. A., Sunyaev R. A., 2007, *Astronomy Letters*, 33, 149
 Ikhsanov N. R., Finger M. H., 2012, *ApJ*, 753, 1
 in't Zand J. J. M., 2005, *A&A*, 441, L1
 Krivonos R., Tsygankov S., Lutovinov A., Revnivtsev M., Churazov E., Sunyaev R., 2012, *A&A*, 545, A27
 Lamers H. J. G. L. M., van den Heuvel E. P. J., Petterson J. A., 1976, *A&A*, 49, 327
 Molkov S., Mowlavi N., Goldwurm A., Strong A., Lund N., Paul J., Oosterbroek T., 2003, *The Astronomer's Telegram*, 176, 1
 Negueruela I., Smith D. M., Reig P., Chaty S., Torrejón J. M., 2006, in *Proc. of the "The X-ray Universe 2005"*, Ed. by A. Wilson. *ESA SP-604*, Vol. 1, 2006, p. 165
 Negueruela I., Torrejón J. M., Reig P., Ribó M., Smith D. M., 2008, in *AIP Conf. Ser.*, Bandyopadhyay R. M., Wachter S., Gelino D., Gelino C. R., eds., Vol. 1010, pp. 252–256
 Oskinova L. M., Feldmeier A., Kretschmar P., 2012, *MNRAS*, 421, 2820
 Paizis A., Sidoli L., 2014, *MNRAS*, 439, 3439
 Pellizza L. J., Chaty S., Negueruela I., 2006, *A&A*, 455, 653
 Puls J., Vink J. S., Najarro F., 2008, *A&AR*, 16, 209
 Rahoui F., Chaty S., Lagage P.-O., Pantin E., 2008, *A&A*, 484, 801
 Rampy R. A., Smith D. M., Negueruela I., 2009, *ApJ*, 707, 243
 Romano P. et al., 2014, *A&A*, 562, A2
 Romano P. et al., 2011, *MNRAS*, 410, 1825
 Romano P., Sidoli L., Cusumano G., Vercellone S., Mangano V., Krimm H. A., 2009, *ApJ*, 696, 2068
 Sguera V. et al., 2005, *A&A*, 444, 221
 Shakura N., Postnov K., Hjalmarsdotter L., 2013, *MNRAS*, 428, 670
 Shakura N., Postnov K., Kochetkova A., Hjalmarsdotter L., 2012, *MNRAS*, 420, 216
 Shakura N. I., Postnov K. A., Kochetkova A. Y., Hjalmarsdotter L., 2013, *Physics-Uspekhi*, 56, 321
 Shakura N. I., Postnov K. A., Kochetkova A. Y., Hjalmarsdotter L., 2014, in *European Physical Journal Web of Conferences*, Vol. 64, p. 2001
 Sidoli L., 2012, in *Proc. 9th INTEGRAL Workshop*. Published online at "<http://pos.sissa.it/cgi-bin/reader/conf.cgi?confid=176>", id.11
 Sidoli L. et al., 2008, *ApJ*, 687, 1230
 Sidoli L., Romano P., Mereghetti S., Paizis A., Vercellone S., Mangano V., Götz D., 2007, *A&A*, 476, 1307
 Sunyaev R. A., Grebenev S. A., Lutovinov A. A., Rodriguez J., Mereghetti S., Gotz D., Courvoisier T., 2003, *The Astronomer's Telegram*, 190, 1
 ud-Doula A., Owocki S. P., 2002, *ApJ*, 576, 413
 Vitrichenko E. A., Nadyozhin D. K., Razinkova T. L., 2007, *Astronomy Letters*, 33, 251
 Walter R., Zurita Heras J., 2007, *A&A*, 476, 335
 Zelenyi L. M., Milovanov A. V., 2004, *Physics Uspekhi*, 47, 1
 Zweibel E. G., Yamada M., 2009, *ARAA*, 47, 291